# Numerical study on effects of coal properties on spontaneous heating in longwall gob areas

Liming Yuan *, Alex C. Smith

*Pittsburgh Research Laboratory, National Institute for Occupational Safety and Health, P.O. Box 18070, Cochrans Mill Road, Pittsburgh, PA 15236, United States*

A B S T R A C T

A computational fluid dynamics (CFD) study was conducted to model effects of coal properties on the potential for spontaneous heating in longwall gob (mined-out) areas. A two longwall panel district using a bleeder ventilation system was simulated. The permeability and porosity profiles for the longwall gob were generated from a geotechnical model and were used as inputs for the three-dimensional CFD modeling. The spontaneous heating is modeled as the low-temperature oxidation of coal in the gob using kinetic data obtained from previous laboratory-scale spontaneous combustion studies. Heat generated from coal oxidation is dissipated by convection and conduction, while oxygen and oxidation products are transported by convection and diffusion. Unsteady state simulations were conducted for three different US coals and simulation results were compared with some available test results. The effects of coal surface area and heat of reaction on the spontaneous heating process were also examined.

## 1. Introduction

Spontaneous combustion continues to be a problem for US underground coal mines, particularly in western mines where the coal is generally of lower rank. From 1990 to 1999, approximately 17% of the 87 total reported fires for US underground coal mines were caused by spontaneous combustion [1]. The risk of an explosion ignited by a spontaneous combustion fire is also present in those mines with appreciable levels of accumulated methane. In fact, three of the mine fires from the reported period resulted in subsequent methane explosions. The incidence of such fires is expected to increase with the projected increased mining of lower rank coals, and the resulting explosion hazard is expected to increase with the projected increased mining of deeper mines (more methane) and the growth in the dimensions of longwall panels (ventilation strain).

Spontaneous combustion of coal occurs when sufficient oxygen is available and when the heat that is produced by the low-temperature reaction of coal with oxygen is not adequately dissipated by conduction or convection, resulting in a net temperature increase in the coal mass. Under conditions that favor a high heating rate, the coal attains thermal runaway and a fire ensues. Spontaneous combustion has also long been a problem in the storage and transport of coal. Much research has been done in experimental study and mathematical modeling of spontaneous combustion of coals as reviewed by Carras and Young [2]. The spontaneous combustion potential of coals can be evaluated qualitatively in a laboratory using one of four commonly used methods: adiabatic calorimetry, isothermal calorimetry, oxygen sorption, and temperature differential methods. Although laboratory results are valuable, their extrapolation to the mining environment has not been completely successful because of complicated scaling effects that cannot be reproduced in small scale experiments. Because of problems in scaling of radiative heat transfer, the small scale spontaneous combustion results will not be able to be scaled to large-scale when coal temperature is high enough that the radiative heat transfer cannot be neglected. For small scale tests in which radiative heat transfer can be neglected (low coal temperature), the test results have also not been validated. The spontaneous heating of coal in mines often occurs in a gob area and is not easily detected. The amount of coal that accumulates in these areas and the degree of ventilation can combine to give favorable conditions for spontaneous combustion. In order to prevent the occurrence of spontaneous combustion in a gob area, it is important to investigate the spontaneous heating of coals under realistic mine ventilation conditions with realistic methane generation and coal chemistry. Because of the very nature and large size of a longwall gob area, it is very difficult to conduct full-scale tests. Thus, numerical modeling is needed to assess spontaneous combustion susceptibility and provide insights for spontaneous heating for different coal properties and ventilation conditions. Such modeling can also be completed in a short time and at comparatively low cost.

Some numerical modeling studies have been done to understand the mechanisms of spontaneous combustion [3–10]. These studies were one or two-dimensional models that mainly focused

* Corresponding author. Tel.: +1 412 386 4961; fax: +1 412 386 6595.
*E-mail address:* Lcy6@cdc.gov (L. Yuan).

on small size coal stockpiles. Little modeling work has been done using actual underground mining conditions. Saghafi et al. did numerical modeling of spontaneous combustion in underground coal mines with a U-ventilation system [11,12], but their work was also limited to two dimensions. Balusu et al. conducted a CFD study of gob gas flow mechanics to develop gas and spontaneous combustion control strategies for a highly gassy mine [13]. In this study, three-dimensional CFD modeling of spontaneous heating of different coals in longwall gob areas was conducted using experimental data obtained by Smith and Lazzara [14] and Smith et al. [15].

## 2. Gob layout and ventilation system

Longwall mining is an exploitation method used in flat-lying, relatively thin tabular coal seams in which a long face is established to extract the coal. In these operations, a mechanical shearer progressively mines a large block of coal, called a panel, which is outlined with development entries or gate roads. The mined coal is then hauled by a conveyor along the length of the face and removed from the mine. The roof is supported by special hydraulic supports and shields that are advanced as the mining progresses. The mine roof is allowed to cave behind in a carefully controlled manner. The caved area is called the gob. The entry on the solid coal block side of the reserve is called the headgate. The headgate is used for the transportation of coal, men, and supplies into and out of the face. The entry on the other side of the panel is used for the passage of return air and is called the tailgate. When the panel entries on both sides have been developed, they are connected by the entries at the end of the panel, called the bleeder entries. A passageway driven between the entry and its parallel course is called the crosscut. The airflow in an entry can be controlled by a regulator that is usually constructed as an opening of adjustable size in a ventilation door. Two types of ventilation systems are used for longwall mining: referred to as bleeder and bleederless ventilation systems. These ventilation systems are designed to keep methane accumulation away from mining activities. In a bleeder system, the gob behind the active face, as well as previous mined-out panels, is kept open and is ventilated to carry away the methane gas from the gob area. In the bleederless system, seals are installed in every crosscut after the panel is mined-out, and the gob is isolated without any ventilation.

A typical longwall district in an underground coal mine may consist of multiple panels. These panels are typically ventilated using bleeder fans to ventilate the active and mined-out panels. In mines with a demonstrated history of spontaneous combustion, bleederless systems may be permitted as a spontaneous combustion control method. In the US, currently only two mines utilize the bleederless system. In this paper, spontaneous combustion with the bleeder ventilation system was studied, while in a later phase of this study, spontaneous combustion with the bleederless ventilation system will be investigated. In this work, two panels are simulated, one as a mine-out panel and the other one as an active panel, utilizing a bleeder system and a bleeder fan. The layout of the two panels and the ventilation system is shown in Fig. 1. Each simulated gob area is 2000 m long, 300 m wide, and 10 m high starting from the bottom of the coal seam. The ventilation airways are 2 m high and 5 m wide. Gob A represents the completed panel, while gob B represents the active one. The ventilation scheme includes a three-entry bleeder system. This ventilation scheme and the panel dimensions are typical of longwall mines operating in the Northern Appalachian Coal Basin of the Pittsburgh coal seam. For western coal mines, the longwall panel layout and ventilation systems may be slightly different from those in Pittsburgh coal seam, but the mechanisms that affect spontaneous heating are the same. The simulation results obtained in this work still address the typical spontaneous heating problems in western coal mines. In the model, it is assumed that the middle entry between gob A and B and an entry on gob A's tailgate side are partially open. All crosscuts between the first and second entries on the headgate side of gob B are open as shown in Fig. 1. The bleeder entries at the back end of the gob are represented as one entry connecting to the bleeder fan for modeling purposes. Fresh air at the intake inlet is separated into four parts. Most of the air enters the face to carry away methane from the working face and returns to the exhaust fan. Some fresh air enters the gob of the active panel B in the headgate side through the second intake entry. Some fresh air travels through the third intake entry to dilute the methane coming from the back ends of panel B and panel A. Gobs B and A are ventilated by the bleeder fan. Except at the face, the air flow in two gobs is towards the bleeder fan. Some fresh air enters the tailgate entry of the panel A to dilute methane coming from gob A. Four regulators are located at the end of the second and third intake entries and two tailgate entries, respectively, for controlling the bleeder ventilation. The detailed ventilation data are described in Section 4.

## 3. Modeling of low-temperature coal oxidation

The chemical reaction between coal and oxygen at low-temperatures is complex. Generally, three types of processes are believed to occur [2]. These are (i) physical adsorption; (ii) chemical adsorption which leads to the formation of coal–oxygen complexes and oxygenated carbon species; and (iii) oxidation in which the coal and oxygen react with the release of gaseous products, typically carbon monoxide (CO), carbon dioxide ($CO_2$), and water vapor ($H_2O$). Of the above processes, oxidation is by far the most exothermic.

The moisture content of coal can play an important role in the low-temperature coal oxidation. The interaction between water vapor and coal can be exothermic or endothermic depending on whether the water condenses or evaporates. Sondreal and Ellman [3] reported that for dried lignite, the rate of temperature increase due to the adsorption of water increased with the moisture content up to a value of 20% water (by mass) and then decreased with further increasing moisture content. Smith and Lazzara [14] found that, initially, the rate of temperature rise depends on the heat-of-wetting. Later the heating curves pass through an inflection point, in which neither the heat-of-wetting mechanism nor the oxidation mechanism dominates. In the final phase, the oxidation mechanism dominates. The effect of the moisture content of the air on the self-heating process was also dependent on coal rank and temperature. Smith and Glasser [16] concluded that adsorption of water vapor does not in itself compete with the low-temperature oxidation in terms of 'heat generation', but appears to speed up the oxidation rate, and possibly plays a catalytic role. The same conclusion was reached by Smith and Lazzara [14]. In underground coal mines, the fresh air is often saturated with moisture before it enters the gob. Although low rank coals usually contain more moisture, these moistures are not able to escape from the coal into the saturated air. Therefore, the effect of moisture on the spontaneous heating of the coal in the gob can be neglected.

The chemical reaction between coal and oxygen is simplified as

$$\text{Coal} + O_2 \rightarrow CO_2 + 0.1CO + \text{heat} \quad (1)$$

The detailed chemical structure of coal varies with the rank and origin of coal. According to experimental data [15], 1 mole of coal reacting with 1 mole of oxygen generates 1 mole carbon dioxide and roughly 0.1 mole carbon monoxide plus heat at the early stage of coal oxidation. These stoichiometric data were for Wyoming No.

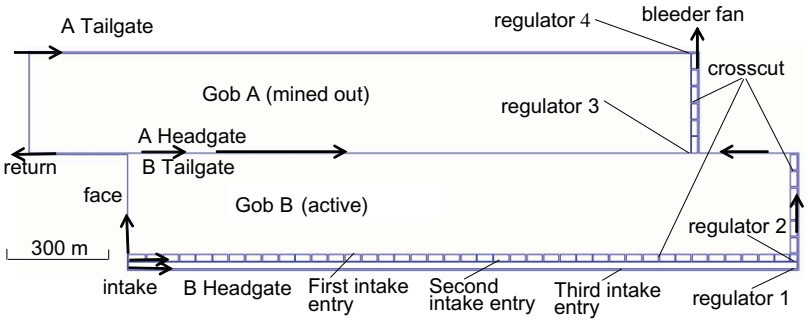


**Fig. 1.** Layout of gob areas and ventilation system.

80 coal. The coal oxidation with oxygen is a type of heterogeneous reaction. The heat of reaction is calculated using heat of formation for reactants (coal), and products ($CO_2$ and CO). The dependence of the rate of oxidation, *r*, on temperature and oxygen concentration can be expressed in the Arrhenius form:

$$r = A[O_2]^n \exp(-E/RT) \tag{2}$$

where the chemical reaction rate is defined as the rate of change in the concentrations of the reactants and products with a unit of kmol/($m^3$ s), A is the pre-exponential factor with a unit of (kmol/$m^3$)$^{1-n}$ $s^{-1}$, *E* is the apparent activation energy with a unit of kcal/mol, *R* is gas constant with a unit of kcal/(mol K), n is the apparent order of reaction, *T* is the absolute temperature in K and $[O_2]$ is the oxygen concentration with a unit of kmol/$m^3$. The value of the apparent order of the reaction, *n*, in low-temperature oxidation studies of coal and other carbonaceous materials has been shown to vary from ~0.5 to 1.0 [2,14], and is about 0.61 for some US coals [17]. Using this value, the reaction rate becomes

$$r = [O_2]^{0.61} A \exp(-E/RT) \tag{3}$$

The heat generated from oxidation is dissipated by conduction and convection while the oxygen and oxidation products are transported by convection and diffusion. The convection in the gob is caused by ventilation that creates a large pressure differential between the intake inlet and the bleeder fan. The detailed pressure values at intake inlet and bleeder fan are described as part of the boundary conditions in Section 4. The early stage of spontaneous heating is a slow process, and the gas and coal particles are assumed to be in thermal equilibrium [2,9]. Therefore, the energy transport equation is written as

$$(\varepsilon\rho_g C_{pg} + (1-\varepsilon)\rho_c C_{pc})\frac{\partial T}{\partial t} + \rho_g C_{pg}\left(u\frac{\partial T}{\partial x} + v\frac{\partial T}{\partial y} + w\frac{\partial T}{\partial z}\right) = \lambda_{eff}\left(\frac{\partial^2 T}{\partial x^2} + \frac{\partial^2 T}{\partial y^2} + \frac{\partial^2 T}{\partial z^2}\right) + rQ \tag{4}$$

where ε is the porosity, $\rho_g$, $C_{pg}$ *are the density and specific heat for the gas,* $\rho_c$, $C_{pc}$ *are the density and specific heat for coal, Q* is the heat of reaction of coal oxidation and $\lambda_{eff}$ is the effective thermal conductivity of coal matrix. This effective thermal conductivity is calculated as

$$\lambda_{eff} = \varepsilon\lambda_g + (1-\varepsilon)\lambda_c \tag{5}$$

where $\lambda_g$ and $\lambda_c$ are the thermal conductivity for gas and coal.

The value of apparent activation energy, *E*, of different coals can very between 12 and 95 kJ/mol. The pre-exponential factor, *A*, depends more on coal rank and measurement method. In this study, the activation energy and pre-exponential factor data obtained by Smith and Lazzara using an adiabatic heating oven were used [14]. In their study, minimum self-heating temperatures for 24 US coal samples were determined and the activation energy and pre-exponential factor were derived using the simple Arrhenius equation

$$\frac{dT}{dt} = A^* \exp(-E/RT) \tag{6}$$

This is a simplified form of Eq. (3). In this equation, the reaction rate, *r*, is represented by the rate of temperature increase, and the zero order reaction is assumed. The activation energy of coal is independent of the order of reaction, while the pre-exponential factor includes the dependence of reaction rate on oxygen concentration. Therefore, the activation energy in Eq. (6) is the same as in Eq. (3), but the pre-exponential factor in Eq. (6) is different from that in Eq. (3). In order to differentiate with the pre-exponential factor *A* in Eqs. (3) and (6), here $A^*$ was used to denote the pre-exponential factor for the zero order reaction, thus it has a unit of K/s. The relationship between *A* and $A^*$ can be obtained by an applying the energy balance equation to coal particles

$$\rho_s C_{ps}\frac{dT}{dt} = Q[O_2]^{0.61} A \exp(-E/RT) \tag{7}$$

where $\rho_s$ is the coal particle density in kg/$m^3$ and $C_{ps}$ *is the coal specific heat in J/(kg K). Substituting Eq. (6) into Eq. (7),*

$$\rho_s C_{ps} A^* \exp(-E/RT) = Q[O_2]^{0.61} A \exp(-E/RT)$$

Thus

$$A = \frac{\rho_s C_{ps}}{Q[O_2]^{0.61}} A^* \tag{8}$$

In order to simulate the spontaneous heating of coal in longwall gob areas, the source and amount of coal needs to be quantified. Coal can be left from the mined coal seam or from other overlying or underlying coal seams. In this study, the coal available in the two gobs is from a 1-m thick rider coal seam that is originally above the Pittsburgh coal seam. After the 2-m thick Pittsburgh coal seam was completely mined-out (no coal left in the gob from this coal seam), the rider coal seam caved into the bottom of the gob. Fig. 2 shows the cross-section of two longwall panels with the caving coal layer at the bottom of the gobs. The spontaneous combustion can occur in this broken coal layer if oxygen is present. In gob B, the air needed for the coal oxidation is from the leakage of ventilation air in the face entry and the second intake entry (the first intake entry collapses and becomes part of the gob). In gob A, the air supporting the oxidation is from the panel A tailgate entry and the leakage from the gob B. Immediately above the broken coal layer is the broken rock that forms the gob and is characterized by gob porosity and permeability distributions. Because the broken rock affects the gob flow, and the heat from coal heating can also transfer to rock through convention and conduction, the entire

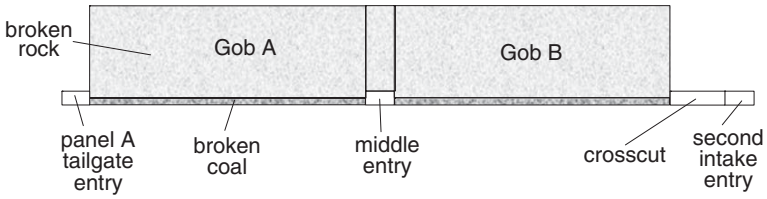


**Fig. 2.** Cross-section of two longwall panels with caving coal layer (not in scale).

**Table 1**
Basic equations solved for gas flow modeling

| | |
|---|---|
| Mass | $\frac{\partial u}{\partial x}+\frac{\partial v}{\partial y}+\frac{\partial w}{\partial z}=0$ |
| Momentum $x$-direction | $\varepsilon\rho(u\frac{\partial u}{\partial x}+v\frac{\partial u}{\partial y}+w\frac{\partial u}{\partial z})=-\varepsilon\frac{\partial p}{\partial x}+\varepsilon\mu(\frac{\partial^2 u}{\partial x^2}+\frac{\partial^2 u}{\partial y^2}+\frac{\partial^2 u}{\partial z^2})-\frac{\mu}{k}u$ |
| Momentum $y$-direction | $\varepsilon\rho(u\frac{\partial v}{\partial x}+v\frac{\partial v}{\partial y}+w\frac{\partial v}{\partial z})=-\varepsilon\frac{\partial p}{\partial y}+\varepsilon\mu(\frac{\partial^2 v}{\partial x^2}+\frac{\partial^2 v}{\partial y^2}+\frac{\partial^2 v}{\partial z^2})-\frac{\mu}{k}v$ |
| Momentum $z$-direction | $\varepsilon\rho(u\frac{\partial w}{\partial x}+v\frac{\partial w}{\partial y}+w\frac{\partial w}{\partial z})=-\varepsilon\frac{\partial p}{\partial z}+\varepsilon\mu(\frac{\partial^2 w}{\partial x^2}+\frac{\partial^2 w}{\partial y^2}+\frac{\partial^2 w}{\partial z^2})-\frac{\mu}{k}w$ |
| Species | $\rho u\frac{\partial Y_i}{\partial x}+\rho v\frac{\partial Y_i}{\partial y}+\rho w\frac{\partial Y_i}{\partial z}=\rho D_i\frac{\partial^2 Y_i}{\partial x^2}+\rho D_i\frac{\partial^2 Y_i}{\partial y^2}+\rho D_i\frac{\partial^2 Y_i}{\partial z^2}+S_i$ |

Here $\mu$ is kinetic viscosity; $k$ is the permeability of the gob, $D$ is the gas diffusion coefficient, $S$ is the rate of species production or consumption.

gob including broken rock and broken coal layer will be modeled. It is assumed that the boundary of the gobs is adiabatic. In addition to the two gobs, all the entries and crosscuts shown in Fig. 1 will also be modeled.

The oxidation of coal will occur on any available coal surface, including both external and internal pore surfaces, with oxygen present. The reaction rate of spontaneous heating of coal in coal stockpiles was found to be related to the external surface area for nonporous coal particles with small pore diameters, and weakly related or not related to particle size for small porous coal particles with larger pore diameters [18]. Nugroho et al. [19] showed that particle size has considerable influence on the self-heating character of coal. While a smaller particle reduces the critical ambient temperature for spontaneous ignition to occur, the product of the exothermicity and the pre-exponential factor QA, and the activation energy of the coals increase with decreasing particle size. Nugroho also reported that change of the critical ambient temperature with particle size is almost negligible for porous coals, but significant for harder, nonporous coals.

It is difficult to define a coal particle size distribution in the coal layer in the gob area because of the large gob size and different caving characteristics in different locations of the gob. The critical parameter that affects the heat generation and dissipation during the spontaneous heating process in the modeling is the coal surface area available in a unit volume, or surface-to-volume ratio. This surface-to-volume ratio value roughly represents an average coal particle size. The surface-to-volume ratio, s/v, for a spherical particle is $6/D$ with $D$ the diameter of the particle, while the surface-to-volume ratio for a unit volume, $S/V$, is $(1-\varepsilon)s/v$ with $\varepsilon$ the porosity of the unit volume. So $S/V = 6(1-\varepsilon)/D$. If an average coal particle diameter of 10 cm is assumed, then the surface-to-volume ratio would be 36/m using a typical porosity value of 0.4 within the uncompacted gob.

## 4. Numerical modeling

In order to simulate spontaneous heating of coal in gob areas, the steady state flow field in gobs was first modeled assuming that the gob consists of only broken rocks. The basic equations solved for the gas flow modeling are listed in Table 1. Then, the break coal layer was added to the bottom of the gob replacing the original broken rock at the same location. When spontaneous heating occurs in the broken coal layer, the steady state flow field will be affected, and becomes unsteady. Because the rock layer above the coal layer affect both the gas flow and heat transfer, the entire gob including both rock and coal layers will be simulated. The air entering the gob form the intake inlet and panel A tailgate is fresh air containing 21% of oxygen by volume. During spontaneous simulations, in addition to unsteady state mass, momentum and species ($O_2$, $CH_4$, CO, $CO_2$) equations, energy Eq. (4) will also be solved.

A commercial CFD software program, FLUENT[1] from Fluent, Inc., was used in this study to simulate the gas flow and spontaneous heating in the longwall gob areas. The gas flow in the longwall mine gob area was treated as laminar flow in a porous medium using Darcy's law, while the gas flow in the ventilation airways was simulated as fully developed turbulent flow. The physical model and mesh for the CFD simulation were generated using the mesh generator software, GAMBIT, from Fluent, Inc. The cell size varies from 1 to 4 m in the model with larger size cells located near the center of the gob. The total cell number was over 1.5 million.

The permeability and porosity distributions of the gob areas were generated using a geotechnical model: FLAC (Fast Lagrangian Analysis of Continua), using the specific geological conditions of a mine in the Pittsburgh coal seam [20]. In the FLAC modeling, mining was simulated in increments, starting from one side of the grid and advancing to the other side. Extraction of the coalbed was modeled by removing elements over the height of the coalbed. The process of gob formation was modeled by first deleting rock elements in the roof of the coalbed, so that they are stress relieved, followed by inserting gob properties in these elements. Gob properties were also inserted in previously mined coalbed elements, so that the gob filled the mined void. The gob properties such as elastic modulus, Poisson Ratio, cohesion and friction angle of different rocks were measured in laboratory tests. The output of the FLAC model is the permeability distribution in the gob. The model was validated using empirical observation of the height of caving. The permeability value varies from $2.97\times10^{-8}$ to $8.42\times10^{-7}$ m$^2$ ($3.0\times10^4$–$8.5\times10^5$ millidarcies), while the porosity value varies from 0.17 to 0.41. Around the perimeter of the gob and immediately behind the face shields, the permeability and porosity values were the largest, while near the center of the gob, these values were the smallest. These permeability and porosity distributions were then input into FLUENT.

Methane emission was also considered in the simulation because it affects the oxygen concentration distribution in the gob. Methane is liberated from the face and inside the gob from the coal remaining within and around the gob. Under normal mining conditions, most of the methane from the gob coal is released in the first several hours, after which the release becomes slow. Since the time period for spontaneous combustion is typically at least several days, the gob coal methane emission is not considered in this simulation. Another source of continuous gob methane emission is from any overlying or underlying coal seam reservoirs. The methane from these coal seam reservoirs is assumed to be released uniformly along the border between the gob and the reservoir. Using

[1] Reference to a specific product is for informational purposes and does not imply endorsement by NIOSH.

ventilation data from a local Pittsburgh coal seam mine, the amount of methane released from the rider coal seam reservoir in this simulation is 0.13 $m^3/s$ (280 cfm) for panel B and 0.024 $m^3/s$ (50 cfm) for panel A. The methane emission rate from the face to the panel B is 0.014 $m^3/s$ (29 cfm). These data were also entered into FLUENT using C subroutines.

The boundary conditions for ventilation pressures used in the simulation were also obtained from a local Pittsburgh coal seam mine's ventilation data. The pressure was −0.7 kPa (−3.0 in. water gauge) at the intake inlet, −0.87 kPa (−3.5 in. water gauge) at the return outlet, and −2.7 kPa (−11.0 in. water gauge) at the bottom of the bleeder shaft. The wall roughness of the ventilation airways was adjusted to have a total intake airflow rate of 41 $m^3/s$ (87,000 cfm) in the active longwall panel. The pressure drops through the two regulators located at the second and third intake entries were also adjusted to have an airflow rate entering onto the face of 28 $m^3/s$ (60,000 cfm). The pressure drop at regulator 3 was adjusted to have a flow rate at the return of 24 $m^3/s$ (50,000 cfm), and the flow rate in the entry on panel A's tailgate side was 3.3 $m^3/s$ (7000 cfm) by adjusting the pressure drop at the regulator 4.

A simulation was conducted first without coal oxidation to obtain steady state flow field and gas distributions. Then, the unsteady simulation with coal oxidation was conducted using the steady state solution as the initial conditions. The longwall face was assumed stationary during the simulation. The physical properties for coal and air as input parameters are listed in Table 2.

**Table 2**
Physical properties for coal and air

| | | |
|---|---|---|
| Coal density | 1300 | $kg/m^3$ |
| Coal specific heat | 1003.2 | J/kg K |
| Coal conductivity | 0.1998 | W/m K |
| Heat of reaction | 300 | kJ/mol $O_2$ |
| Air specific heat | 1.0 | J/kg K |
| Air conductivity | $2.6 \times 10^{-2}$ | W/m K |
| Air dynamic viscosity | $1.8 \times 10^{-5}$ | kg/m s |
| Gas diffusion coefficient | $1.5 \times 10^{-5}$ | $m^2/s$ |
| Initial temperature | 300 | K |

## 5. Flow patterns inside the gob

The flow patterns inside a gob will have a significant effect on the spontaneous heating of coals because the oxygen needed for the oxidation is provided by the gas flow, and the heat generated

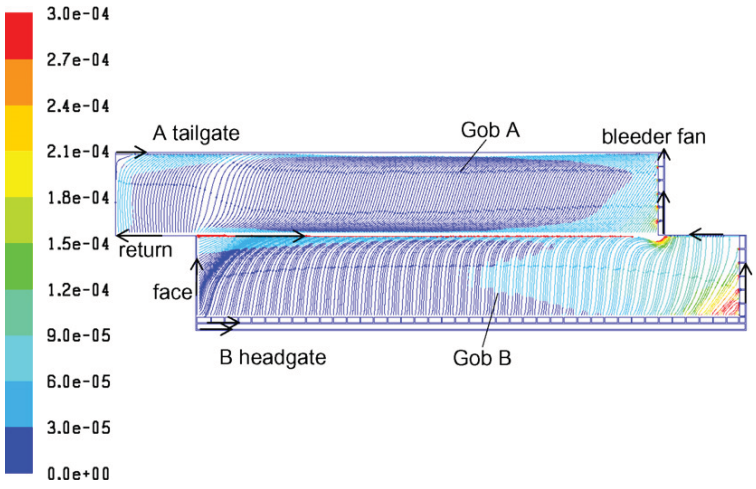


**Fig. 3.** Flow path lines colored by velocity magnitude (m/s) in gob areas.

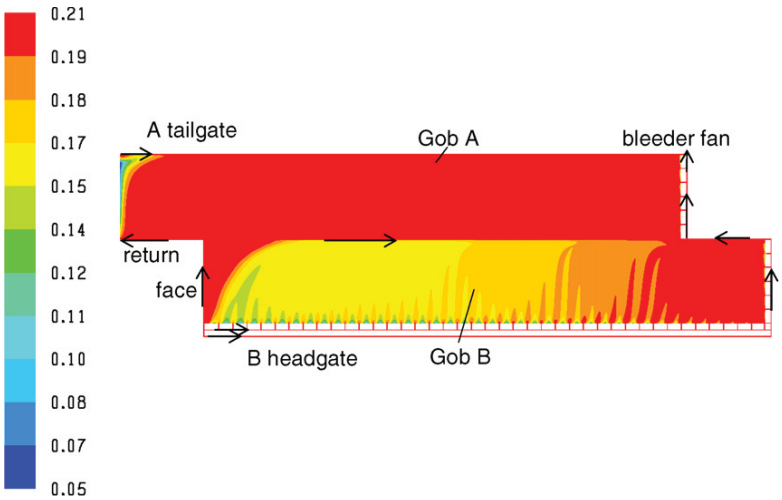


**Fig. 4.** Contours of oxygen concentration (1 = 100%) in gob areas.

from the oxidation may be carried away by the gas flow. The gas flow inside a gob is expected to be three-dimensional with the flow in the vertical direction, but weaker than in the other two directions due to reduced permeability and pressure gradients. In order to visualize the flow patterns inside the gob, a virtual horizontal reference surface was created 1 m from the bottom of the mined seam floor to compare the results with respect to this horizontal reference surface. Fig. 3 shows the flow path lines colored by velocity magnitude in the two gob areas. In the face entry, most air flows from intake inlet to return outlet. Inside the gob, because of pressure differential between the intake inlet and the bleeder fan, air flows from the headgate side to the tailgate side. At the face, air entered into the gob through the gaps between the face shields and flowed to the middle entry between the two panels. The higher gas velocity was between $1.5 \times 10^{-4}$ and $3.0 \times 10^{-4}$ m/s (0.03 to 0.06 fpm) near the back end of panel B. Fig. 4 shows the oxygen distribution in two panels. The oxygen concentration was at 21% in most of mined-out gob A. In the active gob, B, the oxygen concentration close to the intake entry was below 21% because of methane emission from the overlying coal seam reservoir. The openings of crosscuts between the first and second intake entries appear to be very important to dilute the methane concentration near the perimeter of the gob on the headgate side of the active panel. The purpose of opening these crosscuts is to bleed the gob (sweep out the methane). As discussed later, these open crosscuts at same time may facilitate the spontaneous combustion by providing enough oxygen. Therefore, in a bleederless ventilation system, all these crosscuts are completely sealed.

## 6. Simulation results and discussion

Three coals tested by Smith and Lazzara [14] were selected for these simulations as the coal left in the gob areas. Three coals were labeled as No. 80-1, E-1 and Pittsburgh coal, respectively. The adiabatic heating oven test results for these three coal samples are shown in Table 3. Based on the laboratory-scale evaluation, coal sample No. 80-1 has a low minimum self-heating temperature (SHT) and activation energy representing a high tendency for spontaneous combustion. Pittsburgh coal sample has high minimum SHT and activation energy, representing a lower potential for spontaneous combustion. The E-1 coal sample falls in between in terms of spontaneous combustion potential. These values represent a relative spontaneous combustion potential. Under the right conditions, all coals can undergo spontaneous combustion.

Spontaneous heating can begin at ambient temperature when coal is exposed to oxygen. As the self-heating proceeds, the coal temperature increases slowly. The temperature rise usually consists of two stages. The first stage is a slow temperature rise while the second one is a fast temperature rise. The start of the second stage is also called thermal runaway. The time to reach a thermal runaway is called induction time. When the coal temperature reaches about 500 K (230 °C), the spontaneous heating mechanism changes to rapid combustion [21]. So the simulations were focused on the self-heating mechanism at temperatures below 500 K. The surface-to-volume ratio used in the simulations is 36/m, which is equivalent to an average coal particle diameter of 10 cm. Fig. 5 shows temperature and oxygen concentration distributions for the No. 80-1 coal after 10 days. It is apparent that temperature rises occurred in three areas. Area I is the area close to the active tailgate and around the return. Area II is the area nearby the crosscuts and close to the back end of the active panel B, and area III is close to the middle entry and back end of the mined-out panel A. There was very little or no temperature rise in the other areas. This is because oxygen was nearly all consumed by coal oxidation at the periphery of the gob areas and no oxygen was available inside the gobs. This is evidenced by the oxygen concentration distribution in Fig. 5d and indicates that spontaneous heating is mainly controlled by oxygen availability. Under the ventilation conditions studied here, not enough oxygen could be carried to the compressed gob area through convection and diffusion before being consumed on the edges of the gob. The temperature rise rates in three areas were also different. Inside each area, temperature was not uniform. At any time, there existed a maximum temperature in each area. From a fire safety point of view, the maximum temperature represents the worst scenario. Hereafter, the maximum temperature at any time in each area was used to represent the temperature in this area, respectively. Fig. 6 shows the temperatures versus time in three areas. The temperature rises in areas I and III were about 2 days behind those in area II. Fig. 7 shows temperature and oxygen concentration distributions for the E-1 coal after 17.5 days. Temperature rise also occurred only in these three areas mentioned previously. The main difference is that area II had a fast temperature rise after about 14 days, while area I and III were still in the slow increase stage after 18 days with the temperatures below 350 K as shown in Fig. 8. Oxygen was available close to the face, but was depleted very quickly deeper into the gob. Around area II, some oxygen, about 4%, was available, probably accounting for the higher temperature there. Temperature and oxygen concentration distributions for Pittsburgh coal after 40 days are shown in Fig. 9. Higher temperature occurred in areas II and III. Because the temperature rise was very small, 4 degrees, oxygen was available everywhere in the gob areas. This led to slight temperature rises in other areas of the gob.

**Table 3**
Laboratory-scale test results for three coals [14]

| Coal sample | Minimum SHT, °C | *E*, kcal/mol | *A*, K/s |
|---|---|---|---|
| No. 80-1 | 35 | 15.9 | $1.9 \times 10^6$ |
| E-1 | 65 | 17.6 | $1.1 \times 10^7$ |
| Pittsburgh | 90 | 21.1 | $4.4 \times 10^8$ |

### 6.1. Maximum temperature

For all three coals, at any time, area II had the highest temperature. Hereafter, this temperature was referred as the maximum temperature in the gob at given time. Fig. 10 shows the maximum temperature versus time for the three coals using the surface-to-volume ratio of 36/m. For No. 80-1 coal, the maximum temperature rose slowly for the first 5 days. After that it rose very rapidly. For E-1 coal, the maximum temperature rose rapidly after about two weeks. For Pittsburgh coal, after 40 days, the maximum temperature rise was only several degrees. E-1 coal has a minimum SHT that is between those for No. 80-1 and Pittsburgh seam coals. In these simulations, it still reached a thermal runaway, but had a 10 day longer induction time compared with E-1 coal, while Pittsburgh coal does not reach a thermal runaway in 40 days. This indicates that for the same underground mining conditions, a higher laboratory minimum SHT value means that the time to reach thermal runaway is longer.

It should be pointed out that the maximum temperature rise was sensitive to the kinetic properties of the coals: activation energy and pre-exponential factor. The activation energy and pre-exponential factor data were obtained from the laboratory-scale study using very fine coal particles with average diameter between 75 and 150 μm [14]. With larger coal particles, most research has demonstrated that the pre-exponential factor will decrease, but the exact relationship between coal particle size and pre-exponential factor is far from well understood. In a real situation with larger coal particles, the rate of temperature rise will be less than those calculated here. However, the temperature data from this

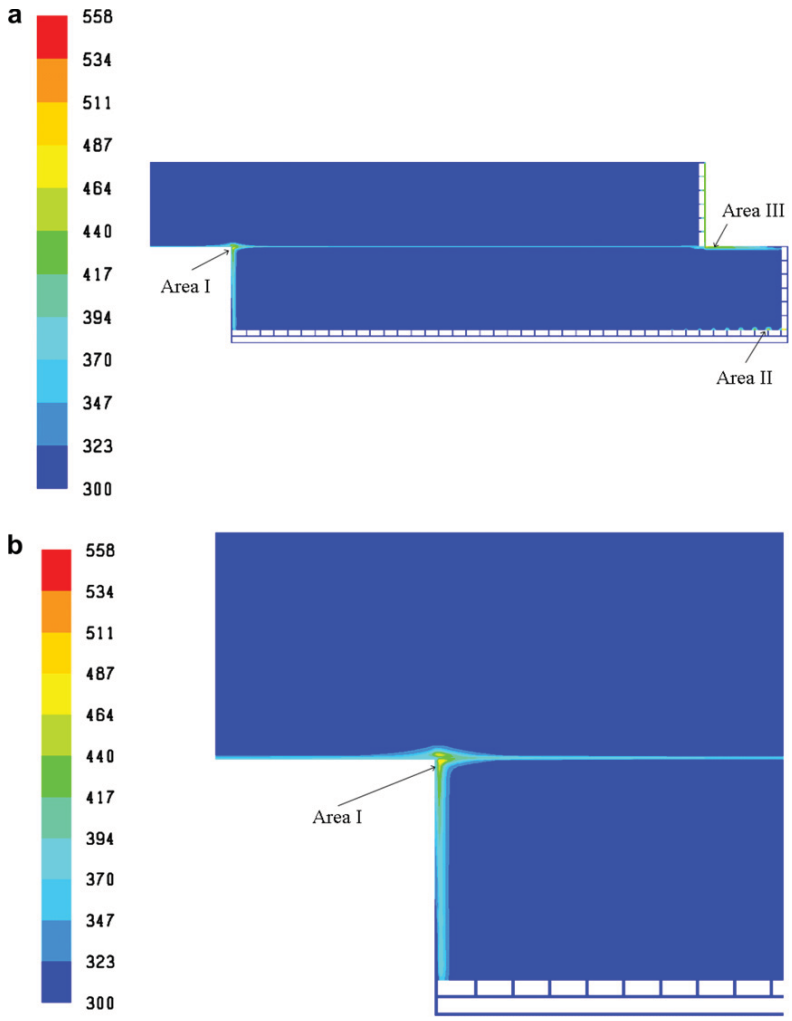


**Fig. 5.** Temperature and oxygen concentration distributions for No. 80-1 coal after 10 days: (a) temperature in entire gob (K); (b) temperature in area I (K); (c) temperature in areas II and III (K); (d) oxygen concentration (1 = 100%).

study can represent results from a worst-case spontaneous combustion scenario.

### 6.2. Comparison with large-scale test results

Smith et al. conducted large-scale studies of spontaneous heating of a large coal mass under conditions that simulate a gob area of a mine [15]. An insulated coal chamber with dimensions of 4.5 m × 1.8 m × 1.8 m was used. The chamber held up to 11,794 kg of coal and was provided with a forced ventilation system. Three experiments were completed using a high-volatile C bituminous coal that exhibited a high spontaneous combustion potential in laboratory-scale tests. In the first two tests, a sustained heating was not achieved. In the third test, temperatures throughout the coalbed increased steadily from the start, with thermal runaway occurring near the center of the coalbed after 23 days. The thermal reaction zone then moved toward the front of the coalbed due to oxygen depletion in the center of the coalbed. The coal used in the third test was the No. 80-1 coal from Table 3. In the experiment, the entire coalbed showed indications of heating immediately after the airflow was started. The temperature histories of the coalbed were recorded using thermocouples arranged in seven vertical arrays 0.3 m, 0.9 m, 1.5 m, 2.1 m, 2.7 m, 3.4 m, and 4.0 m from the front of the coalbed. Each array contained nine thermocouples evenly distributed over the surface along the coalbed width direction. The maximum temperature appeared on one of the thermocouples on the array 0.3 m from the front of the coalbed, the closest one, also because of maximum available oxygen. Fig. 11 shows this maximum temperature history compared with the maximum temperature in gobs obtained from simulations. The temperature rise curves are very similar except that the induction times are different. In the test, it took about 25 days before the thermal runaway occurred. The induction time discrepancy between modeling and test results may be attributed to two factors. First, the dimensions of the large-scale test (4.5 m × 1.8 m × 1.8 m) are far smaller than those for the gob (2000 m × 300 m × 10 m), leading to much lower heat capacity for the coalbed chamber. The sidewalls and floor of the coalbed chamber were insulated with firebricks, while the boundary of the gob was assumed completely adiabatic. Therefore, the relative heat loss from the coalbed chamber boundary was much higher than heat loss from the boundary of the gob (no heat loss), leading to longer time to the thermal runaway. The second factor is the air flow velocity. The average airflow velocity in the coalbed chamber was estimated as about $3.3 \times 10^{-3}$ m/s, while the airflow velocity inside the gob was between $3 \times 10^{-5}$ and $3 \times 10^{-4}$ m/s. The higher airflow veloc-

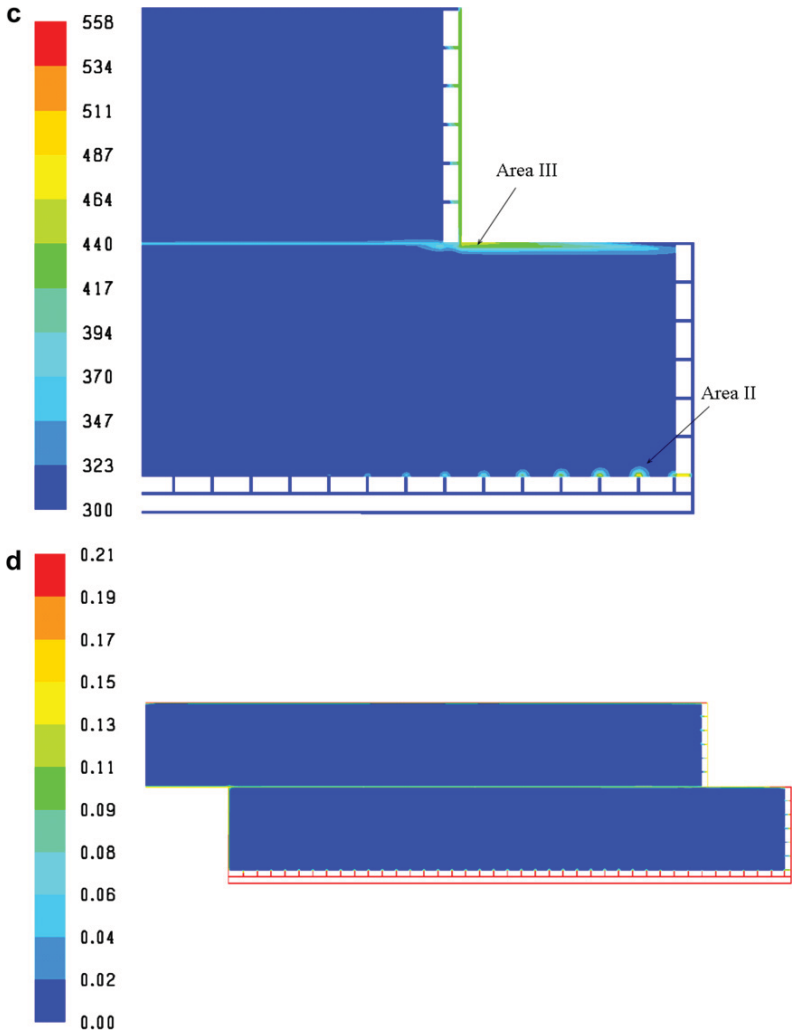


**Fig. 5.** (*continued*)

ity carried away more heat generated from the spontaneous heating, also leading to longer time to reach the thermal runaway. In general, the simulation results are consistent with the test results. More field tests are needed to compare with the modeling results in detail.

### 6.3. Effect of coal surface area

The effect of coal surface area on the spontaneous heating was examined by using different surface-to-volume ratios, $S/V$, for No 80-1 coal. Fig. 12 shows the maximum temperature histories for simulations using three surface-to-volume ratios: 36, 12 and 2 / m. This is equivalent to an average coal particle diameter of 10, 30, and 180 cm, respectively. With $S/V = 2$, the average particle diameter is 180 cm. In reality, this does not indicate a volume with coal particles with a diameter of 180 cm. Instead, it represents a volume with small coal particles coexisting with other non-coal rock particles. When the $S/V$ was reduced to 12/m, not only was the induction time increased to about 17 days, but also the temperature rise in the second stage became less steep, and after about 5 days changed into another slow temperature rise stage, probably because of less heat released in a unit volume. After the $S/V$ was further reduced to 2, maximum temperature rise was only a few degrees in 35 days, and there was no thermal runaway. This indicates that decreasing the coal reaction surface area will greatly reduce the spontaneous combustion fire hazard.

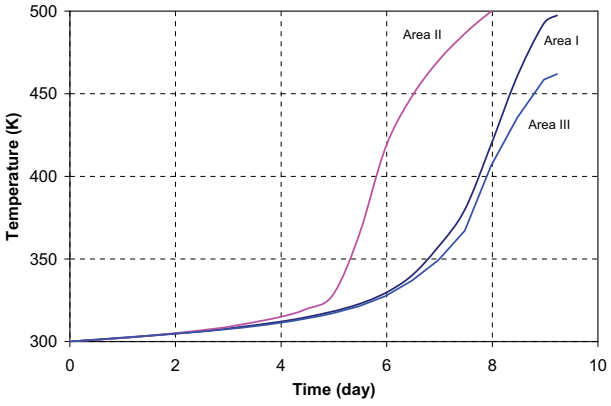


**Fig. 6.** Temperature–time histories in three areas for No. 80-1 coal.

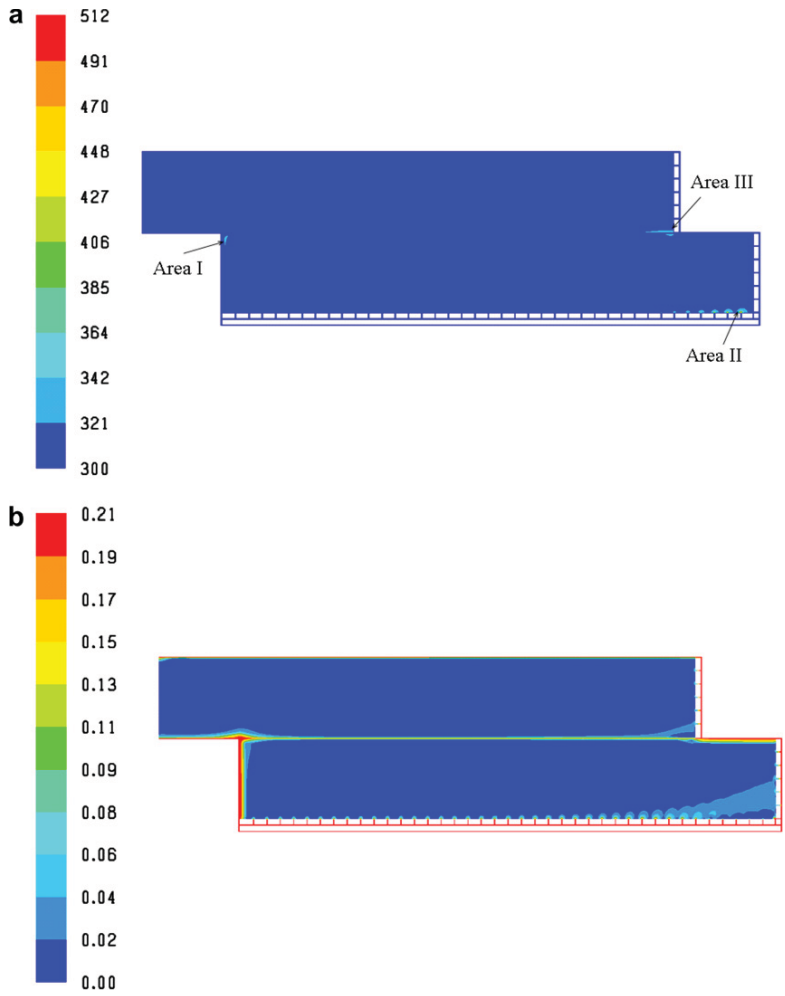


**Fig. 7.** Temperature and oxygen concentration distributions for E-1 coal after 17.5 days: (a) temperature (K); (b) oxygen concentration (1 = 100%)

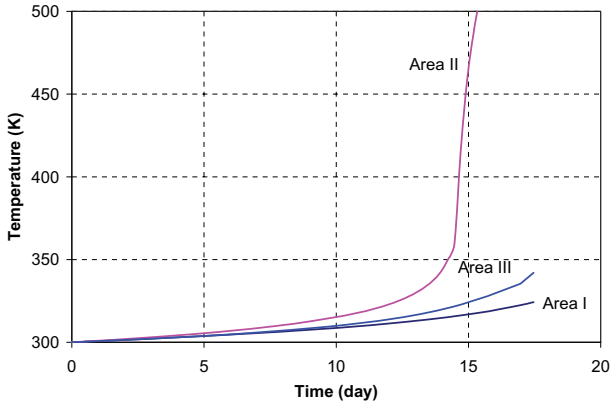


**Fig. 8.** Temperature–time histories in three areas for E-1 coal.

### 6.4. Effect of heat of reaction

Fig. 13 shows simulated maximum temperature histories for coals with different heats of reaction. Three heats of reaction were chosen: $3.0 \times 10^8$, $2.4 \times 10^8$ and $1.6 \times 10^8$ J/kmol $O_2$; roughly equivalent to the heating values of 13,125, 10,500, and 7000 Btu/lb, respectively. The activation energy and pre-exponential values for coal No. 80-1 were used. Coal with a heat of reaction of $3.0 \times 10^8$ J/kmol $O_2$ had an induction time of 5 days, and coal with a heat of reaction of $2.4 \times 10^8$ J/kmol $O_2$ had an induction time of about 7 days. Their maximum temperature–time curves are also very similar. For the coal with a heat of reaction of $1.6 \times 10^8$ J/kmol $O_2$, the induction time increased to about 12 days, and it took about 20 days to reach 500 K, indicating that the heat of reaction of coal oxidation does not have a major effect on spontaneous heating process.

## 7. Conclusions

CFD simulations were conducted to model the spontaneous heating of three coals in longwall gob areas. These coals have different self-heating potentials based on their minimum SHTs evaluated in a laboratory-scale study. Simulation results demonstrate that under typical longwall mining conditions, the spontaneous heating hazards of different coals were strongly dependent on mine ventilation conditions and coal properties. A coal with a larger minimum SHT would result in a longer induction time for spontaneous combustion. Compared with the most active No. 80-1 coal, the E-1 coal's induction time increased by an additional

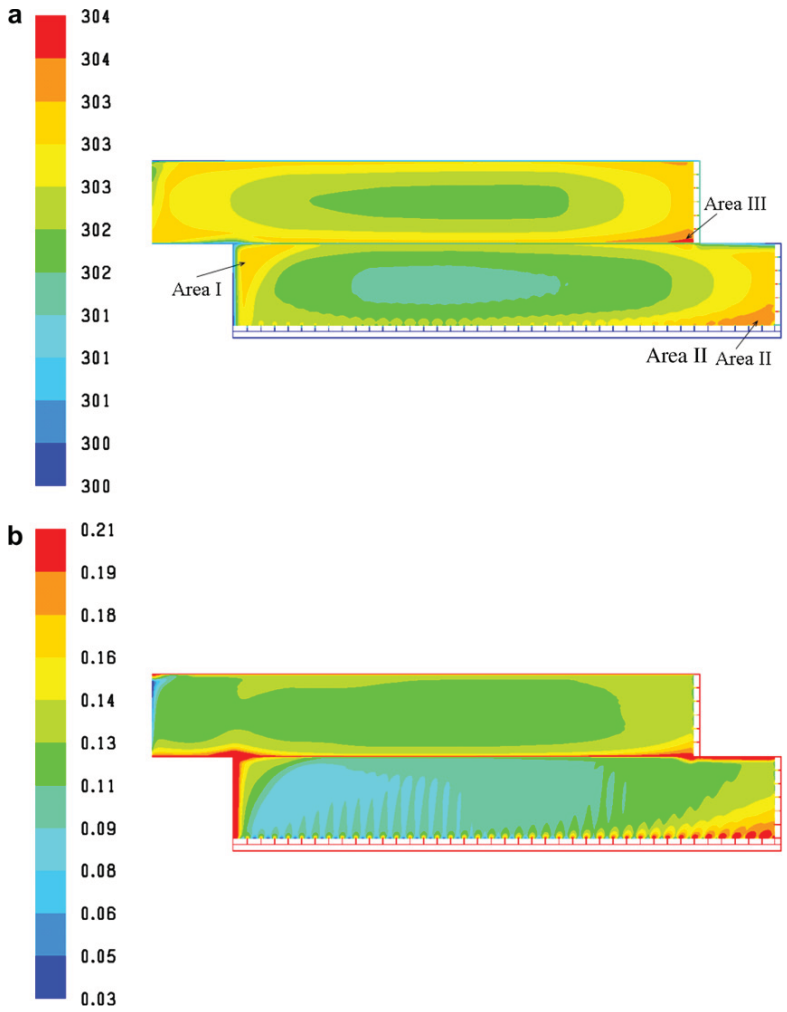


**Fig. 9.** Temperature and oxygen concentration distributions for Pittsburgh coal after 40 days: (a) temperature (K); (b) oxygen (1 = 100%).

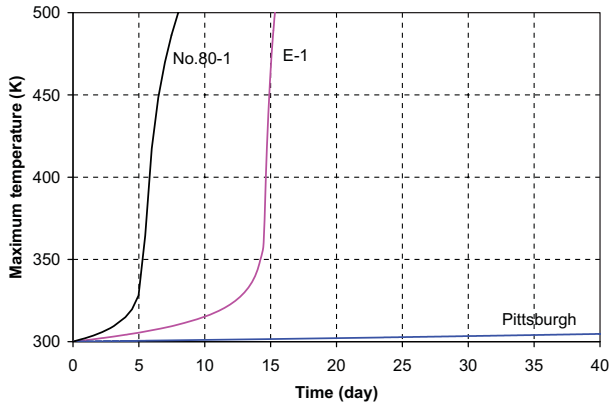


**Fig. 10.** Simulated maximum temperature–time histories in gobs for three coals.

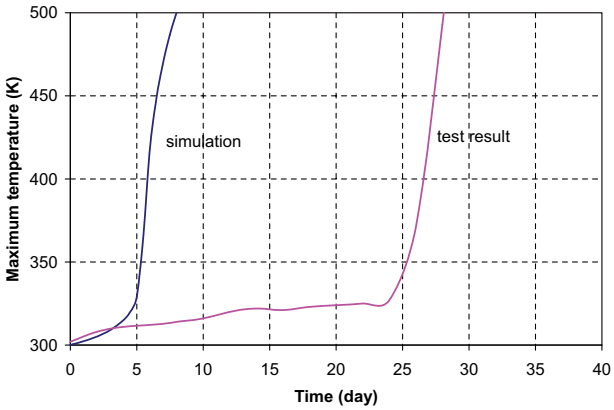


**Fig. 11.** Comparison of maximum temperature–time histories of No. 80-1 coal between simulation and test results [15].

10 days, while for Pittsburgh coal, there was no significant temperature rise in 40 days. The temperature rise occurred in only three areas for No. 80-1 and E-1 coals. The maximum temperature in gobs occurred in area II. For No. 80-1 coal, temperature rise in areas I and III was about two-days behind that in area II, while for E-1 coal, temperature rise in areas I and III was still in the slow increase stage when the temperature in area II was already above 500 K. When the temperature rise was significant, the spontaneous heating became mainly oxygen controlled because oxygen originally present in the gob was consumed by coal oxidation at the early stage.

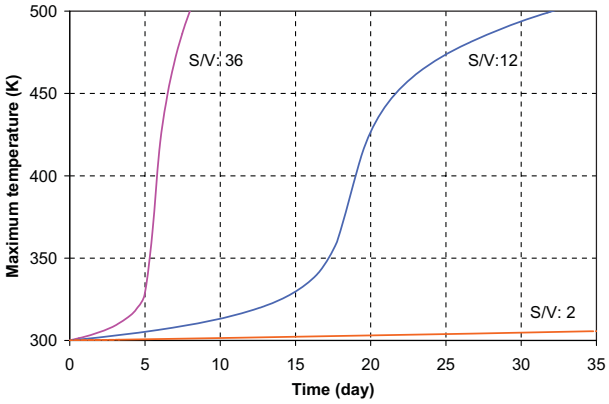


**Fig. 12.** Simulated maximum temperature-time histories for three surface-to-volume ratios: 36, 12 and 2 /m for No. 80-1 coal.

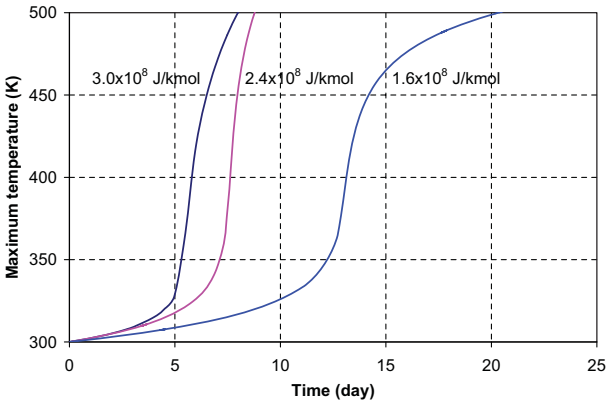


**Fig. 13.** Simulated maximum temperature-time histories for No. 80-1 coal with different heats of reaction.

The temperature rise was greatly dependent on the available coal reaction surface area. For larger coal particle size, the reaction surface area and the maximum temperature rise were both significantly reduced. The heat of reaction of coal oxidation had a minor effect on spontaneous heating. With a lower value of heat of reaction, the induction time was increased but the fire hazard was still present.

In real mining conditions, the face is moving at a certain speed. This movement creates a dynamic flow field that greatly affects the spontaneous heating in the gob area. More research is needed to study the effect of the longwall face movement on the spontaneous heating of coals in the gob areas. Future research also needs to take into account of evaporation or condensation of coal moisture, and the decrease of the rate of oxygen sorption with increasing uptake.

Modeling results from this study are consistent with available large-scale test data except for different induction time. More large-scale test data are needed in the future to further improve the modeling of spontaneous heating in underground gob areas.

## Acknowledgements

The authors wish to acknowledge the technical help from Drs. Gabriel S. Esterhuizen and C. Özgen Karacan with the estimation of permeability and porosity in the gob.

## References

[1] DeRosa M. Analysis of mine fires for all US underground and surface coal mining categories, 1990–1999. National Institute for Occupational Safety and Health Information Circular 9470; 2004.
[2] Carras JN, Young BC. Self-heating of coal and related materials: models, application and test methods. Prog Energ Combust Sci 1994;20:1–15.
[3] Sondreal EA, Ellman RC. Laboratory determination of factors affecting storage of North Dakota lignite. Report of Investigations 7887, US Bureau of Mines; 1974.
[4] Nordon PA. A model for the self-heating reaction of coal and char. Fuel 1979;58:456–64.
[5] Brooks K, Glasser D. A simplified model of spontaneous combustion in coal stockpiles. Fuel 1986;65:1035–41.
[6] Schmal D, Duyzer JH, Van Heuven J W. A model for the spontaneous heating of coal. Fuel 1985;64:963–72.
[7] Arisoy A, Akgun F. Modeling of spontaneous combustion of coal with moisture content included. Fuel 1994;73:281–6.
[8] Rosema A, Guan H, Veld H. Simulation of spontaneous combustion, to study the causes of coal fires in the Rujigou Basin. Fuel 2001;80:7–16.
[9] Edwards JC. Mathematical modeling of spontaneous heating of a coalbed. Report of Investigations 9296. US Bureau of Mines; 1990.
[10] Krishnaswamy S, Agarwal P, Gunn R. Low-temperature oxidation of coal 3. Modeling spontaneous combustion in coal stockpiles. Fuel 1996;75:353–62.
[11] Saghafi A, Bainbridge NB, Carras JN. Modeling of spontaneous heating in a longwall goaf. In: Proceedings of the 7th US mine ventilation symposium; 1995. p. 167–72.
[12] Saghafi A, Carras JN. Modeling of spontaneous combustion in underground coal mines: application to a gassy longwall panel. In: Proceedings of the 27th international conference of safety in mines research institute; 1997. p. 573–9.
[13] Balusu R, Deguchi G, Holland R, Moreby R, Xue S, Wendt M, et al. Goaf gas flow mechanics and development of gas and Sponcom control strategies at a highly gassy mine. Coal Saf 2002;20:35–45.
[14] Smith AC, Lazzara CP. Spontaneous combustion studies of US coals. Report of Investigations 9079. US Bureau of Mines; 1987.
[15] Smith AC, Miron Y, Lazzara CP. Large-scale studies of spontaneous combustion of coal. Report of Investigations 9346. US Bureau of Mines; 1991.
[16] Smith MA, Glasser D. Spontaneous combustion of carbonaceous stockpiles. Part II: Factors affecting the rate of the low-temperature oxidation reaction. Fuel 2005;84:1161–70.
[17] Schmidt LD, Elder JL. Atmospheric oxidation of coal at moderate temperatures. Ind Eng Chem 1940;32:249–56.
[18] Akgun F, Arisoy A. Effect of particle size on the spontaneous heating of a coal stockpile. Combust Flame 1994;99:137–46.
[19] Nugroho YS, McIntosh AC, Gibbs BM. Low-temperature oxidation of single and blended coals. Fuel 2000;79:1951–61.
[20] Esterhuizen GS, Karacan CÖ. A methodology for determining gob permeability distributions and its application to reservoir modeling of coal mine longwalls. In: SME annual meeting, Denver; 2007.
[21] Babrauskas V. Ignition handbook. Issaquash, WA: Fire Science Publishers; 2003.